This is the peer reviewd version of the followng article:

An Enhanced Measuring Instrument for In-Line and Real-Time Blood-pCO2Monitoring using a Custom-Developed Gas-Exchange Filter / Gallerani, A., Muzzarelli, M., Gibertoni, G., Ferrari, A., Cattini, S., Rovati, L.. - In: PROGRESS IN BIOMEDICAL OPTICS AND IMAGING. - ISSN 1605-7422. - 13310:(2025). (Optical Fibers and Sensors for Medical Diagnostics, Treatment, and Environmental Applications XXV 2025 San Francisco 25-31 gennaio 2025) [10.1117/12.3041103].

SPIE
Terms of use:

The terms and conditions for the reuse of this version of the manuscript are specified in the publishing policy. For all terms of use and more information see the publisher's website.

07/11/2026 21:47

(Article begins on next page)

An Enhanced Measuring Instrument for In-Line and Real-Time Blood-pCO_2 Monitoring using a Custom-Developed Gas-Exchange Filter

Alessia Gallerani[a,c], Marco Muzzarelli[a], Giovanni Gibertoni[b], Alberto Ferrari[c], Stefano Cattini[a], and Luigi Rovati[a,c]

[a]Dipartimento di Ingegneria "Enzo Ferrari", Università degli Studi di Modena e Reggio Emilia, Modena, Italy
[b]Dipartimento di Scienze Biomediche, Metaboliche e Neuroscienze, Università degli Studi di Modena e Reggio Emilia, Modena, Italy
[c]Science & Technology Park for Medicine, TPM, Democenter Foundation, Mirandola, 41037 Modena, Italy

ABSTRACT

In this study, we present a low-cost, disposable fluorescent pCO_2 sensor designed for real-time blood pCO_2 monitoring in extracorporeal circulation (ECC) treatments. The sensor consists of a sensitive element enclosed inside a disposable cuvette. The sensor is interrogated by an optical head that, not coming into contact with the blood, can be non-disposable. The heart of the sensor is a gas filter composed of gas-permeable fibers, specifically developed for this application, designed to be low-cost and disposable, ensuring both affordability and convenience for real-time blood-pCO_2 monitoring. The blood in extracorporeal circulation is made to flow through the fibers that, being gas permeable, allow the exchange of gas with the measuring chamber, i.e., the space inside the cuvette outside the fibers, while preventing the exchange of anything that is not gaseous. Inside the measuring chamber, CO_2 exchanged with the blood reacts and modifies the pH of the measuring chamber; this variation is measured thanks to a ratiometric pH-sensitive fluorophore inside the chamber. The fibers used are custom-made polypropylene porous hollow fibers produced using the TIPS technique (thermally induced phase separation) and have a unique structure that allows blood to flow through them. Before being inserted into the cuvette to make the sensor, the produced fibers were fully characterized by optical and scanning electron microscopy (SEM) and their permeability and porosity were also verified. The measuring system thus obtained was verified by simulating a 7-hour extracorporeal circulation treatment using bovine blood and comparing the measurements obtained with those provided by a bench-top blood gas analyzer.

Keywords: Blood pCO_2, biomedical monitoring, biomedical measurement, optical sensors, extracorporeal circulation (ECC), hemodialysis, extracorporeal membrane oxygenation (ECMO), extracorporeal carbon dioxide removal (ECCO2R), heart lung machine, severe acute respiratory syndrome (SARS).

1. INTRODUCTION

The analysis of critical care analytes (CCAs) is of crucial importance for the diagnosis and treatment of severe health disorders, particularly during extracorporeal -blood- circulation (ECC). These analytes include electrolytes (pH, Na^+, K^+, Ca^{2+}, Cl^-), blood gases (O_2, CO_2), and metabolites (glucose, urea, lactate, creatinine).
In this work, we focused on the monitoring of one of these CCAs: blood pCO_2 (partial pressure of carbon dioxide). Carbon dioxide (CO_2) is produced within the body as a result of cellular metabolism. In blood, carbon dioxide exists in three forms: as CO_2 itself, as carbonic acid (H_2CO_3), and as bicarbonate (HCO_3^-). All three forms play a role in the regulation of blood pH, which is typically maintained within the range of 7.35 to 7.45. Due to the narrowness of this range, blood CO_2 levels play a significant physiological role, including the

Further author information: (Send correspondence to Alessia Gallerani)
Alessia Gallerani: E-mail: alessia.gallerani@unimore.it or alessia.gallerani@tpm.bio

regulation of pH, stimulation of breathing acts, and modulation of hemoglobin's affinity for oxygen. Abnormal pCO_2 levels, such as hypercapnia (high pCO_2 levels) or hypocapnia (low pCO_2 levels), are prevalent in critically ill patients[1] and can have significant health consequences, including seizures, coma, or death.
For the in-line and real-time monitoring of blood pCO_2, the analyzing techniques include electrochemical and optical methods like fluorescence and optical absorbance. Also, for real-time monitoring in clinical settings, components of the measuring system in contact with blood must be safe (sterilizable, biocompatible and non-toxic) and disposable in order to avoid complications from cleaning and sterilization. Moreover, they must meet specific metrological performances: accurate CO_2 measurements are essential in a context where physiological normal blood CO_2 ranges from 35 to 45 mmHg, and the accepted clinical error (ΔpCO_2) should be below ± 5 mmHg over a 20-100 mmHg range for long treatments.[2] Also, there are non-essential but desired requirements: avoiding blood sampling and avoiding openings in the bloodline.
In line with the growing employment of ECC treatments, such as extracorporeal membrane oxygenation (ECMO) and extracorporeal carbon dioxide removal (ECCO2R), highly used during the past COVID-19 pandemics, real-time monitoring of blood pCO_2 levels assumes greater significance.
In our recent study,[3] we verified the possibility of measuring in real-time blood pCO_2 in ECC using a measurement system composed of a disposable part, in contact with blood, optically interrogated by an optical head, not in contact with blood and therefore non-disposable. In this study, we investigate the possibility of realizing such disposable part through the use of hollow, hydrophobic, and porous polypropylene (PP) fibers inside the sensor measuring chamber, exploiting the same principle behind ECMO treatments: blood gas exchange via porous hollow fibers.
A key aspect of this work lies in the ability to design, manufacture, and optimize these fibers, tailoring their mechanical and morphological properties to meet pCO_2 real-time and in-line monitoring requirements. Since gas-permeable hollow fiber technology is well-established in the biomedical field, it inherently avoids hemotoxic or hemolytic effects and ensures selective gas exchange without concerns related to leachables. This makes the proposed sensor inherently safe for patient use.
Our goal is to evaluate whether the combination of custom-made hollow fibers, a fluorescent disposable sensor, and a reusable optical head can deliver effective real-time, in-line monitoring of blood pCO_2, meeting the performance and safety criteria outlined above.

2. MATERIALS AND METHODS

2.1 Measuring system description

The proposed instrument is composed of two parts:

- A *disposable, low-cost fluorescent sensor*: this consists of a polycarbonate cuvette containing a bundle of gas-permeable, hydrophobic, and porous PP hollow fibers. These fibers form a membrane that allows blood to flow through while preventing direct contact with the pH-sensitive solution in the outer measuring chamber. The gas permeability of the membrane ensures that, at equilibrium, the pCO_2 levels are identical on both sides of the membrane.

- A *non-disposable optical head*: this component, based on optoelectronic technology, functions as a reading device.

This type of setup allows our system to be mounted directly in line with the ECC system, which also means that the analyte of interest does not require blood sampling. In addition, thanks to the sensor configuration, the optical head is not in direct contact with the bloodstream, meaning that this part is not required to be disposable, while only the disposable part needs to be replaced among different patients, reducing risks, costs, and plastic waste associated with traditional measurement methods.
As introduced previously, the core of the proposed measuring system is the custom-made PP porous hollow fibers produced by means of TIPS technique (thermally induced phase separation). In the following, Subsection 2.2 describes the production and characterization of fibers. Subsections 2.3 and 2.4 describe the proposed measuring system and measurement principle. Finally, Section 2.5 describes the experimental activities performed to verify such a system.

2.2 Hollow fibers production and characterization

2.2.1 Fibers production

The hollow fibers used inside the disposable part of the sensor are produced directly at TPM using the TIPS method.[4] This requires the melting of a polymer, in our case an isotactic PP homopolymer for medical and pharmaceutical injection molding (ELTEX® MED 100-MG03, INEOS, United Kingdom), and a diluent (a mixture of soy and castor oil) to form a homogeneous solution which is then transported via a gear pump to a coaxial nozzle of a spinneret where the hollow fiber exits and undergoes phase separation during the cooling phase. After the extraction of the diluent via conventional solvents, a porous membrane is formed.[4] A scheme of the production process is shown in Figure (1). This allows hollow fibers to be produced from scratch with control over various parameters such as the inner and outer diameters. This is essential because the size of the pores and the thickness of the walls determine fibers permeability to gasses whilst the internal lumen dimensions allow blood to flow smoothly, preventing hemolysis and stagnation phenomena during treatments.

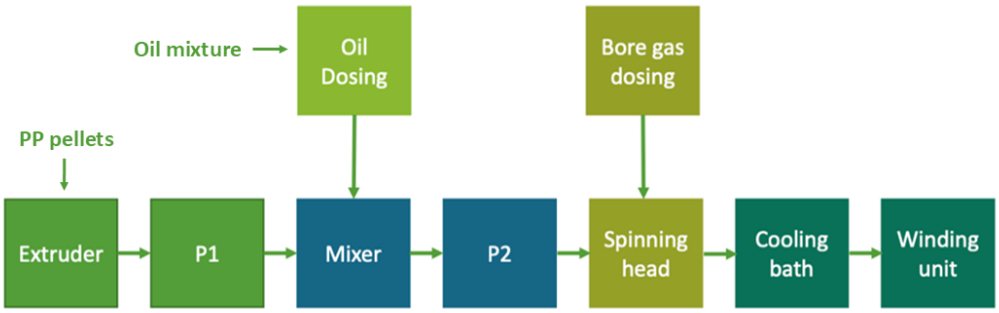

Figure 1: Schematic of the fiber production process. The PP pellets are placed inside the extruder where they melt. Via the gear pump P1, the dope moves inside the mixer, where a homogeneous solution of diluent (a mixture of castor and soybean oils) and PP is created. Then, the P2 pump carries the dope to the spinning head, where a bore gas (nitrogen, N_2) flows, allowing the formation of an hollow fiber. Then the phase separation occurs with fiber passing through a cooling bath. Finally, the fiber is wounded into a bobbin. The dope diluent is then extracted by soaking the bobbins in isopropanol.

2.2.2 Fibers characterization

As introduced earlier, it is necessary to characterize the hollow fibers used for the sensor from a physical point of view. The main characteristics that determine the performance of the fiber are its dimensions (external diameter, internal diameter, and wall thickness) and its porosity, which determines its gas permeability, the principle on which the sensor is based. We used optical microscopy to measure the outer diameter, inner diameter, and wall thickness. With SEM observation, we verified the presence of pores on the outer surface, inner surface, and fiber cross-section, and also estimated their size. We verified the gas permeability by measuring the TMF (Transmembrane Flow) and the porosity using a porometer.

Optical microscope observation:
An initial observation under an optical microscope (Stemi 2000C and SN 51229, Axiocam Erc5, Zeiss, Germany) is the first necessary check to evaluate fiber quality. It allows preliminarily assessing the desired size of the fibers, such as outer and inner diameters and, consequently, wall thickness.

SEM observation:
Observing fibers with a SEM (TM4000 Plus, Hitachi, Japan) allows the view of the internal and external surfaces at higher magnifications and the assessment of the presence of pores on them. To observe a sample, it is necessary to fix the fiber samples on a stub using carbon and copper tape, then partially cut and open the fibers to better appreciate the inner surface characteristics, while the outer surface requires no preliminary preparation.

It is also possible to observe the fibers cross-section: first they must be wet in ethanol and then broken in liquid nitrogen. This allows a "brittle" break to be obtained, which ensures the maintenance of the porous structure within the fiber walls. The samples are then metalized using an Au-Pd target (SC7620 Mini Sputter Coater, Quorum Technologies, United Kingdom) and observed in two modes: secondary electron (SE) and mixed-mode combining backscattered electrons (BSE) and SE, with magnifications up to 6000X.

Transmembrane flow (TMF):
TMF measurement allows to assess the gas permeability of hollow fibers. In our case, we use a dedicated set-up consisting of a 1/4" tube within which a constant pressure is set and maintained using a pressure manometer. A bundle of fibers sample is placed at the end of the tube, and in between the manometer and the sample the presence of a flowmeter allows to measure the airflow exiting from the bundle of fibers. During the measurement increasing values of pressure are chosen (0.6 bar, 1 bar and 1.5 bar). It is possible to estimate the permeability of the fibers, expressed in $mL/cm^2 \cdot min \cdot bar$, by measuring the air flowing through them with the flowmeter. The sample preparation consists of around 20 pieces of fibers 20 cm long fibers forming 20 rings of fibers, gluing the 40 ends together and, after drying, cutting them. This ensures that all fibers are open and that an air flow is allowed to pass through them. To estimate the permeability from the flux measurement we use the following expression:[5]

$$\text{Permeability} = \frac{10^8 \cdot \Phi}{\pi \cdot D \cdot L \cdot n \cdot p}, \tag{1}$$

where Φ is the flux, D is the fiber diameter, L is the fiber length, n is the number of tested fibers and p is the pressure set.

Porometer:
A liquid-liquid porometer (POROLIQ ^{TM} 1000 ML, Porometer, Belgium) is used to estimate different parameters concerning PP hollow fibers pores: the largest pore size (first bubble point, FBP), the mean pore size (mean flow point, MFP) and also the smallest pore size (down to 2 nm). Estimating the pore size is critical because we expect the fiber to exchange only gases, CO_2 in our case. Pores that are too large can allow the passage of even larger molecules than those of interest, such as those contained in the blood, or even the plasma itself, which will wet the fiber and clog it in a short time, making it unusable.

2.3 The proposed measuring system

The working principle we considered in this study is the same we adopted in our previous study.[3,6,7] To measure blood pCO_2, we utilized a principle similar to the Severinghaus design,[8] which incorporates a gas-permeable membrane and electrochemical pH electrodes. Specifically, we use fibers to create a chamber containing a pH-sensitive fluorophore and buffer solution,[6,7] i.e., the measuring chamber. This bundle of fibers prevents the passage of H^+ and other ions but allows CO_2 to be exchanged with the measuring chamber, where it reacts to form H_2CO_3, modifying the pH (increasing/decreasing the H^+ concentration).
Blood pCO_2 is quantified by monitoring the changes in fluorescence of a ratiometric pH-sensitive fluorophore inside the measuring chamber. The pH of the sensing solution can be estimated by analyzing the ratio of fluorescence emissions at 520 nm (λ_{ems}) when the sensing element is excited with light at two wavelengths: $\lambda_{ex-1} = 405$ nm and $\lambda_{ex-2} = 475$ nm. By measuring the emitted fluorescence power, the pH of the sensing solution can be determined, and this pH value is associated with blood pCO_2. The ratiometric pH measurement method has been demonstrated to be highly robust, effectively compensating for variations in both the sensor's geometry and the fluorophore concentration.[9]

2.3.1 Sensor production

The sensor is fully realized in TPM, and this process involves several steps:

- Creation of a fiber bundle: fiber is winded around two pegs fixed at a distance of about 8 cm, creating several windings, paying attention not to pull the fiber.

- The bundle is then placed inside the polycarbonate cuvette and then the overall system is weighted: this step is used to estimate the number of fibers inside the cuvette from which the total exchange area of the membrane can be estimated.
- The ends of the bundle are cut off and the cuvette is then closed with two caps.
- Inside the caps, a two-component polyurethane resin (TEXAFLEX XP 5394 A-HN / XP 5469 B-WS3) is poured onto the ends of the cuvette using a syringe. This allows us to fix the position of the fibers and isolate the measuring chamber from the inside of the fibers.
- The resin curing procedure requires an overnight resting.
- After curing, the caps are removed and the excess resin is cut using a bench-7.3top guillotine (Me-Cut V2.3, Mesep, Poland): this leaves the fibers lumen open, allowing blood to pass through, but preventing blood from entering the measuring chamber.
- After cutting, it is necessary to glue luer-lock adapters to the ends of the cuvette so that it can be connected to the circuit. Again, a two-part polyurethane resin (TEXAFLEX 5397 A - 5538 B) is used.

Using this approach allows blood to circulate through the lumen of the hollow fibers while the measuring chamber is created in the space surrounding the hollow fiber bundle. The cuvette used in this study has ≈ 195 fibers. Then, the chamber outside the fibers is filled with the sensing solution containing a bicarbonate buffer solution (PBS) and a pH-sensitive ratiometric fluorophore. Ratiometric fluorophores are chosen for their reliability in providing accurate measurements.[9,10] We used HPTS (8-Hydroxypyrene-1,3,6-trisulfonic acid trisodium salt), a pH-sensitive, inexpensive, non-toxic, and photostable fluorophore.[11]
A picture of the disposable sensing element completely assembled and containing HPTS solution is shown in Figure (2), and a schematic of its structure and cross-section can be seen in Figure (3).

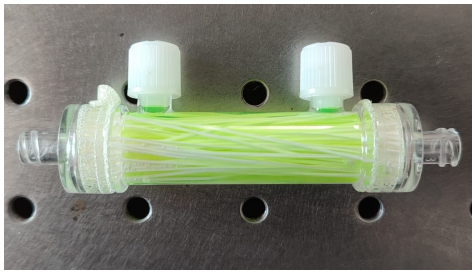

Figure 2: Picture of the ultimated cuvette with hollow fibers. The measuring chamber is filled with HPTS solution.

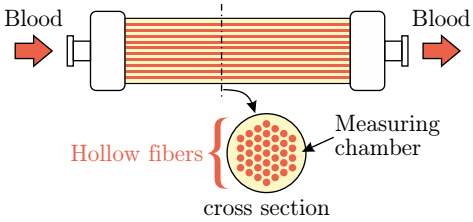

Figure 3: Schematic of the cuvette structure and cross-section.

2.3.2 Non-disposable optical head

A CAD representation of the internal structure of the optical head is shown in Figure (4). The optical head is designed to interrogate the sensor using two different excitation wavelengths, λ_{ex-1} and λ_{ex-2}, while simultaneously recording the optical fluorescence power emitted by the sensing element at the emission wavelength λ_{ems}. The system uses two LEDs (LED1 and LED2) to excite the sensing element, with the optical powers emitted by these LEDs and the fluorescence emitted by the sensing solution measured by two different photodiodes (PD1 and PD2). The currents generated by the photodiodes are processed through transimpedance amplifiers and active filters to obtain output voltages (VPD1 and VPD2). A schematic representation of the optical head layout can be observed in Figure (4). These voltages are digitalized by a data acquisition module (USB-6001 OEM, National Instruments), which also controls the LEDs. A PC, via a Labview graphical user interface (GUI), controls the optical head and provides real-time estimates of the ratiometric signal from fluorophore emission, allowing real-time measurement of blood pCO_2.

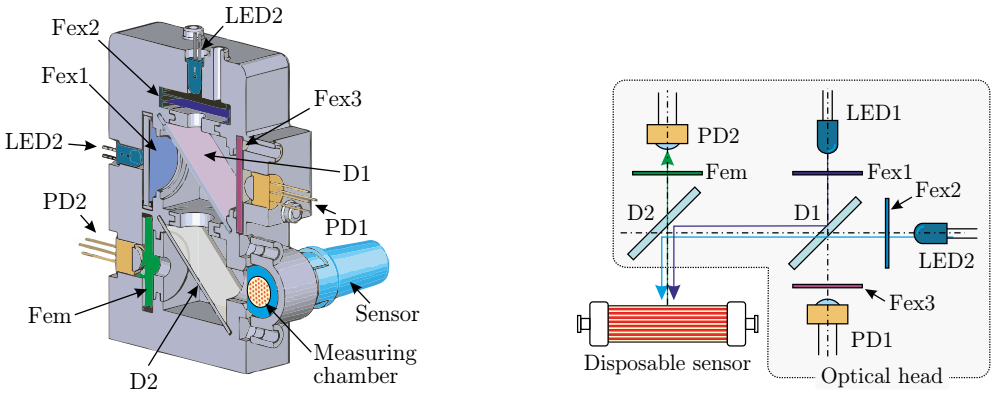

Figure 4: Schematic of the optical head. The light beams produced by the LED1 and LED2 are, respectively, filtered by the excitation filter Fex1 and Fex2 to allow the radiation of only the desired excitation wavelengths. Then, the filtered beams are guided on the sensor exploiting the dichroic mirrors D1 and D2. The photodiode PD1 measures the optical power of the excitation beams produced by LED1 and LED2. The filter Fex3 is aimed at equalizing the optical powers incident on PD1 when LED1 or LED2 are alternately switched ON. The fluorescence optical power produced by the sensor can cross the dichroic D2, thus reaching the photodiode PD2. The emission filter Fem is aimed at filtering out any residual excitation optical power before it reaches PD2.

2.4 Model and measurement protocol

The gas-permeable membrane inside the cuvette allows the sensing element to exchange CO_2 with the patient's blood. The variations in the pH sensing solution are associated with pCO_2 fluctuations through the following reaction:

$$CO_2 + H_2O \leftrightharpoons H_2CO_3{}^- \leftrightharpoons H^+ + HCO_3{}^-, \tag{2}$$

where HCO_3^- represents bicarbonate. The gas-permeable membrane within the cuvette enables the sensing element to exchange CO_2 with the patient's blood, ensuring that the pCO_2 of the blood is in equilibrium with the pCO_2 of the sensing solution in a steady state. This means that the sensor recorded values agree with the pH changes of the HPTS solution and therefore with the changes in pH of the HPTS solution hence with the pCO_2 changes. The relationship between pH and pCO_2 is shown by the following expression:[12]

$$[H^+] = \zeta \cdot pCO_2 \Rightarrow pH = -\log_{10}(\zeta \cdot pCO_2), \tag{3}$$

where ζ includes the solubility coefficient of CO_2 in the buffer, the first acid dissociation constant of $H_2CO_3^-$, and the concentration of HCO_3^- in the sensing element. Once the steady state condition is reached, the pH of the measuring chamber is then determined by pCO_2 in the blood in the extracorporeal circulation. Therefore, by measuring the pH in the measuring chamber, it is possible to estimate the pCO_2 in the blood.
The estimation of the pCO_2 value is based on the calculation of the ratio between the two emissions from the fluorophore solution when excited with the two LEDs. The optical head apparatus measures the fluorescence intensity at 520 nm as voltage signals, which are then corrected for dark signals (V_{dark}) and normalized against the excitation signal (V_{exc}), both of which are evaluated for every acquired sample. This ratio is defined as follows:

$$R = \frac{I_{405}}{I_{465}}, \tag{4}$$

where I_{405} and I_{465} are respectively:

$$\begin{aligned} I_{405} &= \frac{V_{ems_{405}} - V_{dark}}{V_{exc_{405}} - V_{dark}} \\ I_{465} &= \frac{V_{ems_{465}} - V_{dark}}{V_{exc_{465}} - V_{dark}} \end{aligned}. \tag{5}$$

In equation 5, $V_{ems_{405}}$ and $V_{exc_{405}}$ are the voltage signals detected respectively by PD2 and PD1 when LED1 is on, and $V_{ems_{465}}$ and $V_{exc_{465}}$ are the voltage signals detected respectively by PD2 and PD1 when LED2 is ON.

The voltage signals from the emission (V_{ems}) measured by PD2 and excitation (V_{exc}) measured by PD1 depend on the pH-dependent fluorescence intensity and the characteristics of the electronics. The emission signal estimates the optical power of the fluorescence, while the excitation signal compensates for the LED power drift. The dark signal (V_{dark}) compensation in equation 5 is aimed at compensating the effects of both electrical and optical offsets.
Thus, as shown in our previous work,[6,7,10] the ratiometric signal can be related to the pH of the indicator. Provided that the buffering solution (PBS) within the measuring chamber can maintain the pH variations of the sensing element close to its pK_a value (~ 7.3), the pH of the sensing element is linearly related to the ratio R:

$$\mathrm{pH} = \alpha' \cdot R + \beta'. \tag{6}$$

Consequently, the pCO_2 level in blood can be estimated by considering both equation (3) and equation (6), obtaining:

$$\mathrm{pCO_{2-est}} = f(R) = \alpha \cdot 10^{-\beta \cdot R} + \gamma, \tag{7}$$

where pCO_{2-est} represents the estimated pCO_2 value provided by the developed measuring instrument, and α, β and γ are constants that depend also on α' and β' from equation (6).
The instrument was tested using bovine blood and a GEM PREMIER 4000 (Werfen, Italy) hemogas analyzer as a reference system. As shown in Figure (5), the blood pCO_2 was adjusted using a gas exchanger (oxygenator) with a mixture of compressed air, CO_2 and N_2, while the blood temperature was maintained at 36.8 °C using a heat exchanger.
The prototype sensor used for testing allows limited blood flow. To verify its performance inside an ECC line for cardiac surgery, a bypass line was inserted as shown in Figure (5): in this way, the sensing element only receives the blood flow it can tolerate without creating excessive pressure that would cause the module to break.
Blood samples were taken periodically during acquisition exploiting two accesses, site A and site B, see Figure (5). After the optical head warm-up, the developed measuring system recorded $N = 15$ measurements for each pCO_2 value.

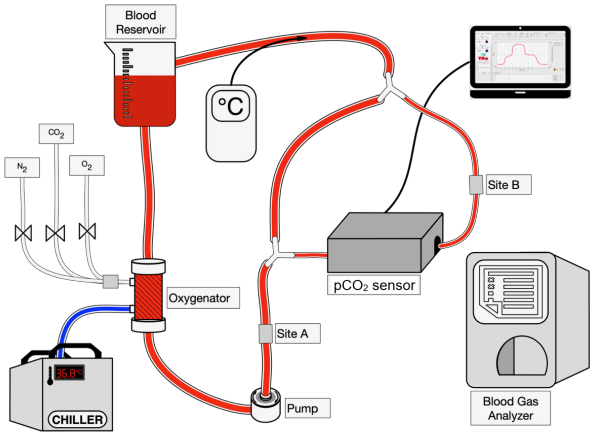

Figure 5: Schematic of the blood circuit employed during the acquisition. The oxygenator and the flow of N_2, CO_2 and O_2, allowed to change their presence in the blood. The chiller made it possible to keep the temperature of the blood constant at 36.8 °C. The pump allowed to control the blood flow rate in the circuit. Blood samples were taken from sites A and B and then analyzed with the hemogas analyzer.

2.5 Experimental verification

To evaluate the proposed blood pCO_2 measurement device, a ≈ 7 hour ECC treatment was simulated using bovine blood. Blood was circulated and maintained at 36.8 °C, with pCO_2 varying in a range between 10 and 120 mmHg. The pCO_2 values estimated by the instrument were compared with those of the reference system based on blood samples. The conditions for the *ex-vivo* tests are summarized in Table 1.

***Ex-vivo* test conditions**	
Blood type	Bovine blood
Blood temperature	36.8 °C
Blood flow	1 L/min
Warm-up time (optical head)	2 h
Test duration	≈ 7 hours
Sampling period	0.5 Hz

Table 1: Experimental test conditions employed during the measurements session.

3. RESULTS AND DISCUSSION

3.1 Fibers physical characterization

3.1.1 Optical microscopy analysis

The observation of fibers cross-section through optical microscopy allowed to assess the value of the inner (d_{in}) and outer (d_{out}) diameters, as shown in Figure (6).

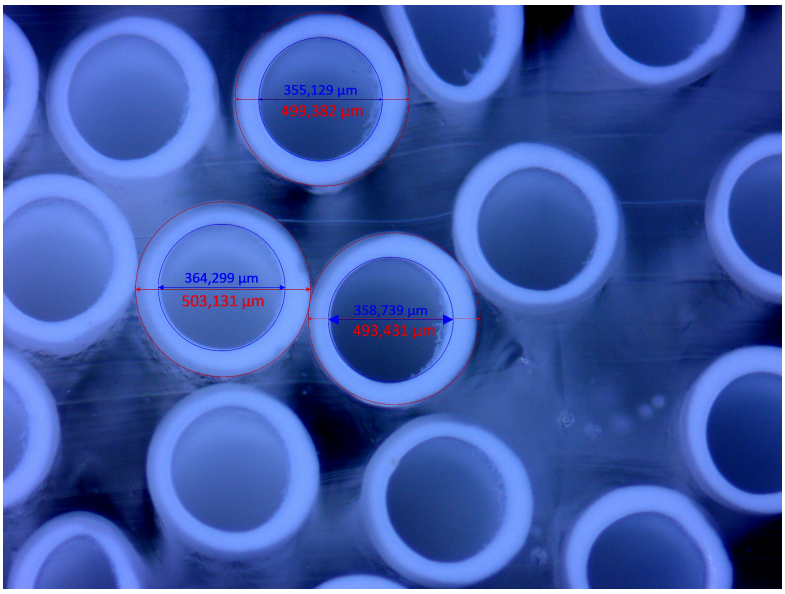

Figure 6: Optical microscope image showing the internal structure of fibers. Inner and outer diameter lengths are measured.

The two diameters were determined by calculating the mean of the measured values, obtaining:

$$d_{in} = 359 \pm 5 \ \ \mu\text{m}$$
$$d_{out} = 499 \pm 5 \ \ \mu\text{m}$$

3.1.2 SEM analysis

Figure (7) shows SEM micrographs of the external and internal surfaces, as well as the cross-section of the fibers used in this study, at magnifications of 1000X, 3000X, and 6000X, respectively.

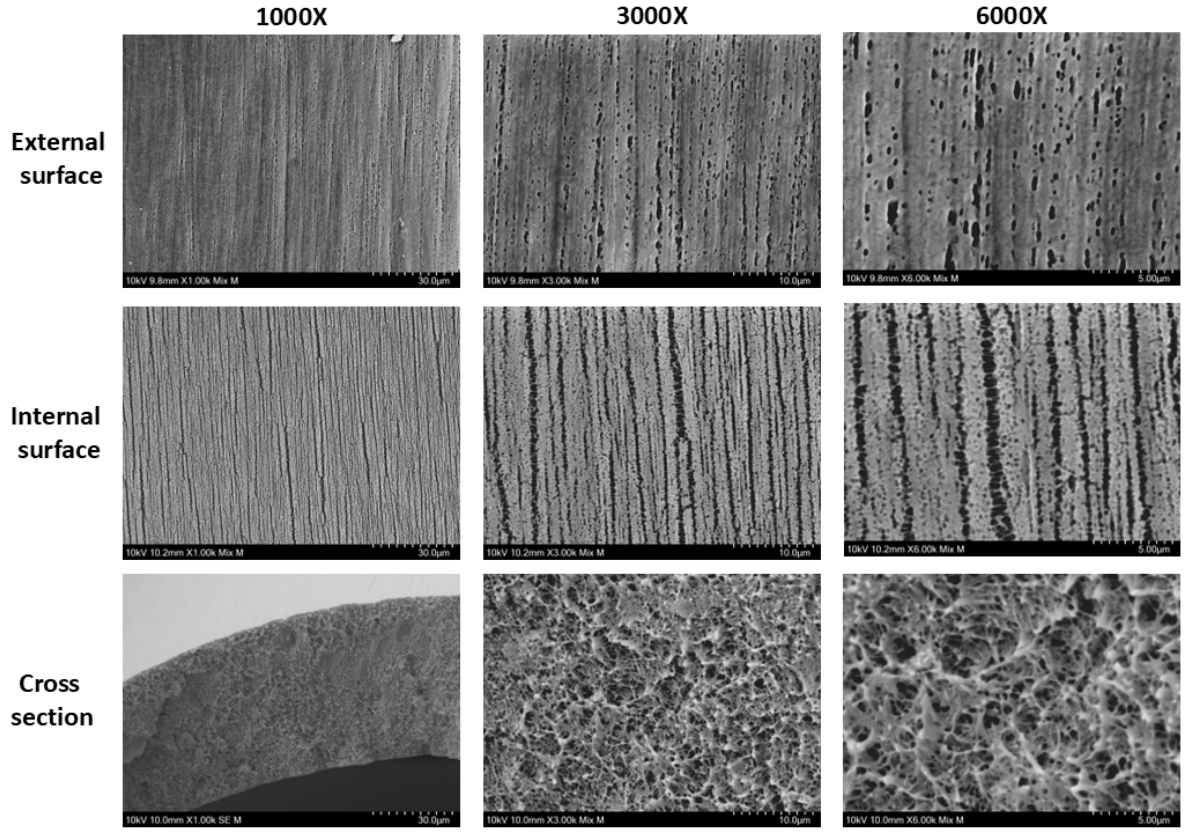

Figure 7: SEM micrographs of a fiber at different magnifications (1000X, 3000X and 6000X). In the first line: the fiber external surface; in the second line the internal surface; in the third line the fiber cross-section.

In the first row of Figure (7), the fiber external surface can be observed. As magnification increases, the presence of pores can be appreciated, showing a mainly vertical orientation and different sizes that vary in a range from about 250 nm to about 1 μm. The second line shows the internal surface of the fiber. Here the porosity is greater than that on the outer surface, again the pores have a vertical orientation and different sizes that vary in a range between 400 nm and 645 nm. The third row shows the fiber cross-section obtained by a rupture in liquid nitrogen. This allows us to see the internal structure of the fiber and also the wall thickness, which measures 56 μm. The fiber presents a sponge-like internal structure with pores of different sizes ranging from 480 nm to 1.15 μm. This allows the exchange only of gases, but not of other elements, such as blood constituents or red blood cells.

It is important to note that SEM measurements allow the measurement of pores but are mainly aimed at analyzing morphology, the actual pore size and therefore the porosity of the fibers is estimated using the porometer.

3.1.3 TMF analysis

Through the TMF measurement, the gas permeability of the fibers is evaluated by measuring the air flux passing through them at different pressure values. The results obtained are presented in Table (2). For this analysis, we considered $n = 20$ fibers with $D \approx 360$ μm and $L = 205$ mm.

Pressure (bar)	**Flow (L/min)**	**Permeability (mL/cm^2·min·bar)**
0.6	1.0	36.0
1.0	1.4	30.0
1.5	2.0	29.0

Table 2: Permeability values measured at increasing values of pressures.

Then, taking the values given in the table, the average permeability value P_{mean} was then calculated:

$$P_{mean} = 32 \pm 3 \ \frac{\text{mL}}{\text{cm}^2 \cdot \text{min} \cdot \text{bar}}.$$

3.1.4 Porometer analysis

Every measurement was performed three times on the same sample. The values obtained are reported in Table (3):

FBT (nm)	**MFP (nm)**	**Smallest pore (nm)**
89,25	54.45	38.29
99.67	68.64	29.89
88.61	55.78	29.82

Table 3: Porometer measurement outputs.

From these repeated measurements, we then estimate the average value of each of the parameters given in Table (3). The average values found are given below:

$$\begin{aligned} \text{FBT} &= 93 \pm 6 \text{ nm} \\ \text{MFP} &= 60 \pm 8 \text{ nm} \\ \text{FBT} &= 33 \pm 5 \text{ nm} \end{aligned}$$

As can be seen, porometer analysis can recognize pores of smaller sizes than those measured with SEM micrographs. This leads us to conclude that the measurement that actually best describes the porosity of the fiber is indeed the porometer, while the SEM allows us to observe the morphology, even the cross-section, but without giving us precise indications on the porosity. Thus, the porometer remains the instrument that provides the most important information that then influences fiber performance during the blood measurement session.

3.2 Experimental results

The pCO_{2-est} values measured by our instrument during the *ex-vivo* test, together with the corresponding pCO_{2-ref} values obtained by the reference instrument, are shown in Figure (8). As shown in the figure, the pCO_{2-est} values are in good agreement with the values measured by blood gas.

Errors between the reference value (pCO_{2-ref}) and the estimated value (pCO_{2-est}) were evaluated using the following relation:

$$\Delta\text{pCO}_2 = \text{pCO}_{2-\text{ref}} - \text{pCO}_{2-\text{est}}. \tag{8}$$

These errors are shown in Figure (9). As illustrated in the figure, when the change in blood pCO_2 occurs too rapidly, the measurement error can exceed the ± 5 mmHg tolerance. This is likely due to the time required

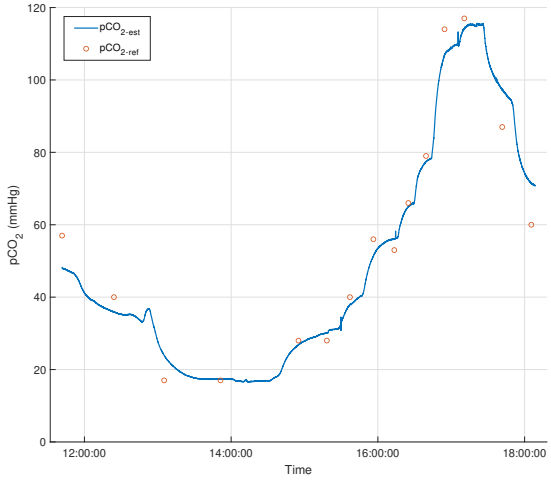

Figure 8: pCO_{2-est} values measured during the *ex-vivo* test (blue line) and the relative pCO_{2-ref} values (red dots) estimated by the reference measuring instrument.

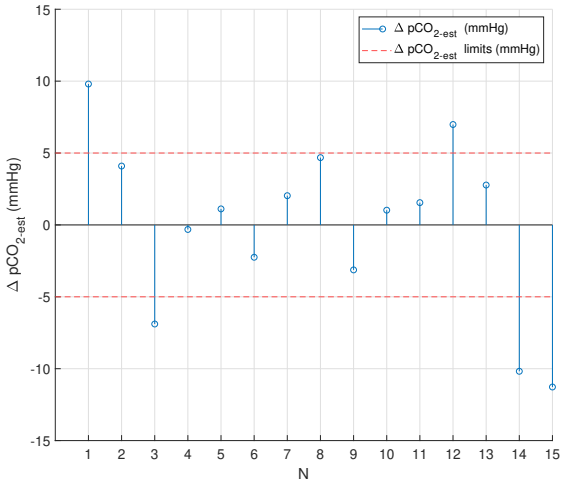

Figure 9: Errors obtained by calculating ΔpCO_2 (blue line). The red dashed lines show the upper and lower limit of tolerance ($\pm$ 5 mmHg) discussed in section (1).

for the sensor to reach equilibrium with the blood. However, it is important to note that the response time is dependent on the exchange surface area. Therefore, increasing the exchange surface area by adding more fibers would also accelerate the response time and reduce the dynamic error.

4. CONCLUSIONS

The analysis of blood pCO_2 is critical for the diagnosis and treatment of critical diseases, especially during ECC. Abnormal pCO_2 levels, which are common in critically ill patients, can lead to serious consequences such as seizures, coma, or death. For this reason, the possibility of measuring this CCA in real-time and in-line during ECC treatments could lead to many advantages, including the possibility of predicting clinically significant changes in pCO_2 levels, thus allowing early intervention and preventing the worsening of patient health. In our previous study, we proposed a pCO_2 measuring system based on a disposable sensor whose operation is based on the use of a gas-permeable membrane.[3] This device, in addition to meeting all the necessary requirements not discussed in section 1, showed excellent performance in measuring blood pCO_2.
In this study, we verified the possibility of realizing the sensor based on the same operating principle as the previous one, using the innovative TIPS technology. The possibility of realizing the sensor using such technology would bring significant advantages in terms of:

1. Full control over the physical characteristics of the filter and, therefore, the performance of the sensor. This is also due to the use of different techniques to characterize the fibers, both from a morphological point of view and in terms of porosity (the most important characteristic) and gas permeability.

2. Absolute biocompatibility, since the use of hollow and porous fibers is already a well-known and widespread technology in the biomedical field. It prevents hemotoxic or hemolytic effects and allows only gas exchange, eliminating concerns about leachable materials. Therefore, we can say that the sensor we tested is safe for the patient.

The fiber was fabricated and characterized using optical microscopy and scanning electron microscopy (SEM). Its porosity was assessed with a porometer and gas permeability was evaluated by measuring the transmembrane flow (TMF).
Following the characterization, a cuvette was constructed using the fibers and filled with a pH-sensitive solution, serving as the disposable component of the sensor. The sensor was then tested in a 7-hour bovine blood

measurement session, during which blood parameters were varied by introducing CO_2 and O_2 gases. A hemogas analyzer was used to assess the consistency and response time of the device.
In conclusion, this study demonstrates that by combining the previously developed pCO_2 measurement technology[3] with the TIPS-based technique for manufacturing hollow PP fibers, we have successfully created a pCO_2 sensor that performs effectively during measurement sessions of duration comparable to those typically encountered in ECC treatments in clinical settings, while meeting all the essential requirements.

ACKNOWLEDGMENTS

We would like to thank Dinamica Generale, Poggio Rusco (MN), Italy, for supporting the experimental activities. The project was funded by the National Recovery and Resilience Plan (NRRP), Mission 04 Component 2, Investment 1.5 - NextGenerationEU, Call for Tender No. 3277 dated 30/12/2021, Award Number: 0001052 dated 23/06/2022 (PNRR MUR Project ECS_000033_ECOSISTER).

REFERENCES

[1] J. Marhong and E. Fan, *"Carbon dioxide in the critically ill: Too much or too little of a good thing?"* Respiratory Care, vol. 59, no. 10, pp. 1597–1605, Oct. 2014. [Online]. Available: http://rc.rcjournal.com/content/59/10/1597.

[2] Centers for Medicare & Medicaid Services, Proposed Rules 42 CFR Part 493. (2019). *"Clinical Laboratory Improvement Amendments of 1988 (CLIA) Proficiency Testing Regulations Related to Analytes and Acceptable Performance"*. [Online]. Available: https://www.govinfo.gov/content/pkg/FR-2019-02-04/pdf/2018-28363.pdf

[3] S. Cattini, L. Accorsi, S. Truzzi and L. Rovati, *"A Measuring Instrument for In-Line and Real-Time Measurement of Blood-pCO_2 in Extracorporeal-Circulation"*, in IEEE Transactions on Instrumentation and Measurement, vol. 69, no. 8, pp. 5640-5648, Aug. 2020, doi: 10.1109/TIM.2019.2961499.

[4] Oğuz Orhun Teber, Ayşegül Derya Altinay, Seyed Ali Naziri Mehrabani, Reyhan Sengur Tasdemir, Bihter Zeytuncu, Esra Ateş Genceli, Ebru Dulekgurgen, Kerem Pekkan, İsmail Koyuncu, "*Polymeric hollow fiber membrane oxygenators as artificial lungs: A review"*, Biochemical Engineering Journal, Volume 180, 2022, 108340, ISSN 1369-703X, https://doi.org/10.1016/j.bej.2022.108340.

[5] Yuanhui Tang, Fanchen Zhang, Fangyu Wu, Lin Wang, Aoxing Feng, Lixin Yu, Huanhuan Wu, Yakai Lin, Xiaolin Wang, "*A novel tunable polypropylene hollow fiber membrane with gradient structure for extracorporeal membrane oxygenation applications,*"Journal of Membrane Science, Volume 693, 2024, 122325, ISSN 0376-7388, https://doi.org/10.1016/j.memsci.2023.122325.

[6] S. Cattini, L. Accorsi, S. Truzzi, and L. Rovati, *"On the development of an instrument for in-line and real-time monitoring of blood-pH in extracorporeal circulation,"* IEEE Trans. Instrum. Meas., vol. 69, no. 8, pp. 5640–5648, Aug. 2020, doi: 10.1109/TIM.2019.2961499.

[7] D. Goldoni, A. Ferrari, M. Piccini, S. Cattini, R. Molinari and L. Rovati,*"Blood-pH Optical Measurement: A Model to Compensate for the Effects of Temperature,"* in IEEE Transactions on Instrumentation and Measurement, vol. 72, pp. 1-8, 2023, Art no. 4003008, doi: 10.1109/TIM.2023.3250282

[8] J. W. Severinghaus and A. F. Bradley, J. *"Electrodes for blood pO_2 and pCO_2 determination"*, Appl. Physiol., vol. 13, no. 3, pp. 515–520, Nov. 1958, doi: 10.1152/jappl.1958.13.3.515.

[9] H. R. Kermis, Y. Kostov, P. Harms, and G. Rao, *"Dual excitation ratiometric fluorescent pH sensor for noninvasive bioprocess monitoring: Development and application"*, Biotechnol. Prog., vol. 18, no. 5, pp. 1047–1053, Oct. 2002. [Online]. Available: https://onlinelibrary.wiley.com/doi/abs/10.1021/bp0255560

[10] S. Cattini, S. Truzzi, L. Accorsi, and L. Rovati, *"Performances and robustness of a fluorescent sensor for nearly-neutral pH measurements in healthcare"*, IEEE Trans. Instrum. Meas., Apr. 1, 2020, doi: 10.1109/TIM.2020.2984964.

[11] I. Johnson and M. Spence, Eds., *"pH indicators"*, in *Molecular Probes Handbook—A Guide to Fluorescent Probes and Labeling Technologies*, 11th ed. Life Technologies, 2010, ch. 20. [Online]. Available: http://www.thermofisher.com/handbook

[12] J. W. Parker et al., *"Fiber-optic sensors for pH and carbon dioxide using a self-referencing dye"*, Anal. Chem., vol. 65, no. 17, pp. 2329–2334, Sep. 1993, doi: 10.1021/ac00065a027.